Environmental Science & Technology

pubs.acs.org/est

Article

Using the Black Carbon Particle Mixing State to Characterize the Lifecycle of Biomass Burning Aerosols

Arthur J. Sedlacek, III,* Ernie R. Lewis, Timothy B. Onasch, Paquita Zuidema, Jens Redemann, Daniel Jaffe, and Lawrence I. Kleinman

Cite This: *Environ. Sci. Technol.* 2022, 56, 14315−14325

Read Online

ACCESS | Metrics & More | Article Recommendations | Supporting Information

ABSTRACT: The lifecycle of black carbon (BC)-containing particles from biomass burns is examined using aircraft and surface observations of the BC mixing state for plume ages from ∼15 min to 10 days. Because BC is nonvolatile and chemically inert, changes in the mixing state of BC-containing particles are driven solely by changes in particle coating, which is mainly secondary organic aerosol (SOA). The coating mass initially increases rapidly (k_{growth} = 0.84 h^{-1}), then remains relatively constant for 1−2 days as plume dilution no longer supports further growth, and then decreases slowly until only ∼30% of the maximum coating mass remains after 10 days (k_{loss} = 0.011 h^{-1}). The mass ratio of coating-to-core for a BC-containing particle with a 100 nm mass-equivalent diameter BC core reaches a maximum of ∼20 after a few hours and drops to ∼5 after 10 days of aging. The initial increase in coating mass can be used to determine SOA formation rates. The slow loss of coating material, not captured in global models, comprises the dominant fraction of the lifecycle of these particles. Coating-to-core mass ratios of BC particles in the stratosphere are much greater than those in the free troposphere indicating a different lifecycle.

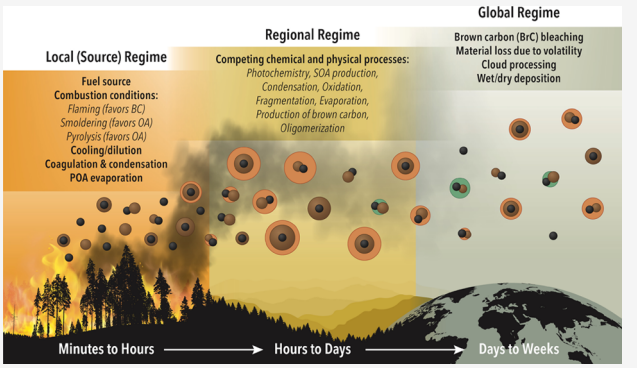

KEYWORDS: *biomass burning aerosols, black carbon, mixing state, aerosol evolution, aerosol lifecycle*

1. INTRODUCTION

Biomass burning (BB) events (i.e., wildfires) are a natural and important part of ecosystems; they remove dead or decaying matter, releasing nutrients back into the soil, and they thin out forest canopies and undergrowth, enabling seedlings to germinate. These events are also an important source of particulate matter in the atmosphere, and the resulting biomass burning aerosol (BBA) influences regional and global climates[1] as well as impacts human and wildlife health.[2−4] With BB events increasing in both intensity and frequency[5,6] due to droughts brought about by increasing global temperatures and changing hydrological cycles, and projected to still further increase,[7,8] a better understanding of BB emissions[2,9] and the evolution of BBA is critical for improving predictions of their impacts on climate, climate change, and human health and for evaluating potential mitigation strategies (e.g., geoengineering[10]).

An important component of BBA is black carbon (BC), which is the largest particulate climate warming agent. BB events account for ∼40% of the atmospheric inventory of this aerosol type.[1,11] Whereas BC comprises only a small fraction of the BBA particulate emission mass, it is responsible for most of the light absorption.[1] Therefore, understanding the microphysical and optical properties of BB−BC particles and the evolution of these properties is of particular importance with regard to climate and climate change.[12]

BC particles emitted by BB events rapidly—within 1−2 h—accumulate large amounts of substances, referred to as coatings. These coatings are mostly organic, and thus the growth rate of the coatings is related to the rate of secondary organic aerosol (SOA) formation. The ratio of the mass of this coating to that of the BC—here termed the "mixing state"—exerts a strong effect on the particle's optical and hygroscopic properties.[13] These coatings can be removed through evaporation and/or chemical processing via the production of more volatile substances, but because BC is nonvolatile and chemically inert, the mass of BC in an individual particle remains constant throughout the particle's lifetime (barring coagulation, which is generally negligible except very near the source). As a consequence, BC can serve as a tracer, and changes in the mixing state of BB−BC-containing particles will be due entirely to changes in the amount of coating material.

Received: July 6, 2022
Revised: September 14, 2022
Accepted: September 15, 2022
Published: October 6, 2022

Table 1. Synopsis of Biomass Burns

	BBOP	MBO	ORACLES	LASIC
estimated age	∼1−3 h	∼12 h	2−12 days	1−2 weeks
age estimation	pseudo-Lagrangian transects	HYSPLIT	WRF-AAM model	HYSPLIT
sampled region	NW-US	NW-US	African coast	mid-Atlantic
nominal lat./lon.	lat: 47.5−42.5 N	lat: 43.98 N	lat: 1−13 S	lat: 7.97 S
	lon: 123−113 W	lon: 121.69 W	lon: 5 E − 14.35 W	lon: 14.35 W
fire emissions	wildfires	wildfire	wildfires/ deforestation	wildfires/ deforestation
fuel source	timber, grass, conifer	conifer, scrub	savannah/ forest[7,50]	savannah/ forest[7,50]
sampled time frame	July−Sept. 2013	August 2016	Aug. 2017/Oct. 2018	June−Sept. 2017
BC geometric mean diameter (nm); i.e., GMD of lognormal fit to $dN/d\log D_{BC,med}$ and geometric standard deviation	118−125 nm	119 nm	117−121 nm	112−130
	1.4−1.7	1.3	1.4−1.6	1.3−1.6

While this quantification does not preclude changes in the chemical (and thus hygroscopic) properties of the particles, it does, nonetheless, capture important information on the evolution of the optical properties through changes in the microphysical properties. In this way, the mixing states of BC-containing particles can be used to investigate atmospheric aging processes (e.g., SOA formation and heterogeneous oxidation) and BBA evolution and radiative forcing.

Due to the complexity and number of processes involved in BB−BC particle formation and evolution, global climate models are forced to distill the microphysical, chemical, hygroscopic, and optical properties and processes of these particles into simple and computationally efficient parameterizations. The bases for these distillations are typically either field studies that have targeted near-source emissions and evolution or laboratory-based studies that have focused on quantifying the influence of one particle property on another (e.g., morphology on particle optical properties or chemical composition on hygroscopicity). However, such parameterizations implicitly imply that BB−BC particle properties do not continue to evolve at longer times or else that this evolution can be accurately extrapolated from measurements procured early in the aerosol lifecycle. To validate such assumptions, measurements of BB−BC mixing state and optical properties at longer times are required.

Direct investigation of the evolution of BB emissions and thus the mixing state of BB−BC particles, such as by a Lagrangian experiment that follows these emissions for extended periods (days to weeks), would be invaluable in characterizing the lifecycle of these particles. However, current studies typically cover only small fractions of this lifecycle and therefore investigations of the evolution of BB−BC particles and their mixing states require measurements from different BB events, potentially at different geographical locations.

Here, we discuss the lifecycle of BBA in the free troposphere derived from measurements of the mixing states of BB−BC particles at different plume ages (i.e., times since emission) ranging from less than an hour to more than a week taken during multiple field campaigns conducted at different locations in the mid-latitudes. These measurements provide a coherent picture of the evolution and lifecycle of the BB−BC particle mixing state, from which the optical properties of these particles and their impacts on radiative forcing can be determined. They also allow quantitative determinations of growth and loss rates of coating mass and have implications for BBA evolution and SOA formation more generally. Our results demonstrate that the microphysical properties (and correlated optical properties) of coated BC particles are continually evolving throughout their lifetimes, with potentially profound impacts on their global reach, human health, and climate forcing.

Due to the immense variety of combustion intensities, fuel sources, and prevailing meteorology, the lifecycle described here, though capturing essential features, will vary between fires in detail that can be determined only by further measurements. Cloud processing, including wet deposition, can play a large role in the subsequent lifecycle of BBA for those emissions that remain in the planetary boundary layer (PBL). Additionally, some extreme BB events can inject particles into the upper troposphere and stratosphere, where they will experience very different environments and undergo very different processes and evolution than those that remain primarily in the free troposphere. Thus, it is unlikely that a one-size-fits-all approach to resolve a "typical" lifecycle of BBA, and, in particular, of BB−BC particles and their properties, can be realized. Nonetheless, it is expected that the lifecycle of BB−BC particles from many BB events that remain primarily in the free troposphere will be similar to that described here, as they will undergo similar processes that affect their mixing states.

2. RESULTS AND DISCUSSION

2.1. Temporal Evolution of BC Mixing State. Information on the field campaigns and experimental details can be found in the Methods section in the Supporting Information (SI). In brief, the mixing states of BB−BC particles were determined by the single-particle soot photometer[14] (SP2; Droplet Measurement Technologies), which measured the mass of the BC contained in individual particles over the range of ∼75−500 nm mass-equivalent diameter ($D_{BC,med}$) and the time-dependent light scattering from individual particles in the diameter range of ∼175−450 nm, from which the mass of the nonrefractory coating of thickness T_{coat} is derived (Figure S1). As determination of the BC mixing state is limited by the narrower range of the scattering measurements, we examine the mixing state for BC particles with $D_{BC,med}$ = 100 nm, which corresponds to a BC mass of ∼1 femtogram. This value yields robust retrievals and is a typical size for BB−BC particles. The quantity used to examine the temporal behavior of the mixing state of BB−BC particles is

https://doi.org/10.1021/acs.est.2c03851
Environ. Sci. Technol. 2022, 56, 14315−14325

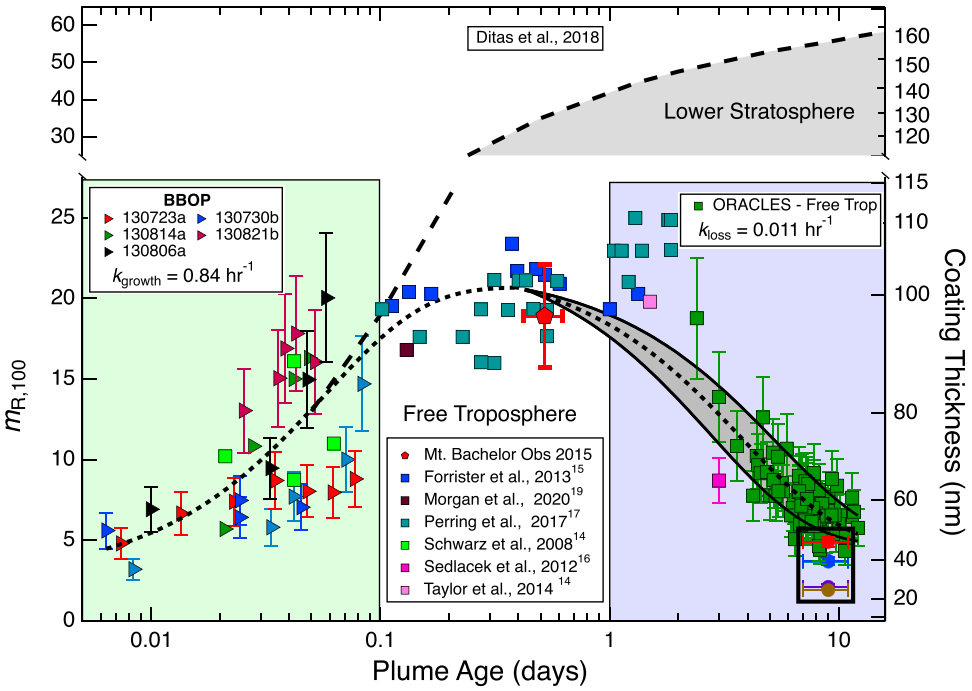

Figure 1. Mass ratio of nonrefractory coating-to-BC for particles with $D_{BC,med}$ = 100 nm, $m_{R,100}$, as a function of plume age. The uncertainties in estimated plume ages for the LASIC data set (delineated by a black box in the lower-right corner) reflect limitations of HYSPLIT-derived air mass ages for this region of the world. The LASIC data were not used in coating loss curve fit due to the presence of boundary layer (cloud) processing biasing the derived $m_{R,100}$ values. Not shown is a single point in Taylor et al.[20] due to uncertainty in plume age. The gray-shaded region captures loss rate constants that are within 50% of k_{loss}. The right axis is the corresponding coating thickness of a 100 nm core, $T_{coat,100}$, for an assumed concentric core−shell particle morphology. Dotted lines are fits described in the text. Shaded rectangles are designed to serve as a rough guide delineating the three regimes. The upper panel is a schematic of the ratio of mass of coating to that of BC for particles with $D_{BC,med}$ = 100 nm, $m_{R,100}$, as a function of the estimated plume age for lower stratospheric BB−BC particles. The rate of coating growth used to derive the estimated increase in $m_{R,100}$ for stratospheric BB−BC (dotted line) is based on the measured increase in the coating thickness of the BC-containing particle sampled from a pair of back-to-back intercontinental flights, as reported by Ditas et al.[61]

the ratio of the average of the coating masses to BC core mass for particles with a 100 nm mass-equivalent diameter BC core, $m_{R,100}$.

Values of $m_{R,100}$ determined from measurements taken during the various field campaigns (listed in Table 1), along with estimates derived from the literature for other tropospheric mid-latitude plumes,[14−19] are shown in Figure 1 as a function of plume age on a logarithmic scale. Separate analyses of the 2013 Rim fire reported both a nearly constant coating thickness[15] [blue squares] and an increase in coating thickness[17] [aqua green squares] to ∼40 hours of aging. Other values, such as those of Taylor et al.[20] from the CLARIFY campaign (their Figure 3C), are consistent but are not plotted due to uncertainty in plume age. Values from the LASIC field campaign, which were determined from measurements in the boundary layer during which particles may have undergone cloud processing, are shown in Figure 1 in a black rectangular box in the lower-right corner, with bounds denoting the youngest and oldest ages. Although these ages were determined by HYSPLIT and are thus less robust than those for which the plumes always remained in the free troposphere (because of the paucity of measurements of the meteorological fields to drive HYSPLIT in the boundary layer[21]), the results are consistent with the general picture obtained from the measurements taken during the other field campaigns.

Initially, $m_{R,100}$ increases rapidly, attaining values of 15−20 within the first few hours following emission, primarily due to the availability of coemitted condensable species that form SOA and to a lesser extent from coagulation with other BC-containing particles and with primary organic aerosol (POA) particles. As dilution and concomitant lower number concentrations quickly relegate coagulation to a secondary role, further coating growth occurs only through condensation, implying that most of the BC coating is secondary in nature.

The values of $m_{R,100}$ during the first 3 hours are represented by an expression for a simple first-order growth model in which $m_{R,100}$ initially increases linearly with time but then approaches a constant value

$$m_{R,100}(t) = m_{R,100_{max}}(1 - e^{-k_{growth}t}) \quad (1)$$

with $m_{R,100,max}$ = 20 and k_{growth} = 0.84 h^{-1} (Figure 1). This formulation corresponds to an initial rate of mass increase of 16 fg h^{-1} for particles with $D_{BC,med}$ = 100 nm (or ∼25 nm coating h^{-1}). Using a condensation model (Supporting Information) where all particles at a given sampling location have experienced the same vapor pressure history with respect to the coating material precursors and all BC particles exhibit a concentric core−shell configuration and possess a lognormal number distribution ($dN/d\log D_{BC,med}$) with a geometric mean diameter of 117 nm and a geometric standard deviation of 1.48, the total mass of coating divided by the mass of total BC for the ensemble, $m_{R,tot}$, is estimated to be 0.35$m_{R,100}$. The core−shell assumption, in which a spherical BC core encapsulated by a coating of uniform thickness, is expected to accurately capture the optical properties because of the large coating thicknesses, i.e., very large values of $m_{R,100}$. The rate

https://doi.org/10.1021/acs.est.2c03851
Environ. Sci. Technol. 2022, 56, 14315−14325

constant for $m_{R,tot}$ will be the same as that for $m_{R,100}$, and thus its initial growth rate will be near 6 h^{-1}. As BC mass does not change, k_{growth} provides a quantitative measure of SOA production. Although not dealt with here, the knowledge of the fraction of the aerosol mass that is bound to BC would provide insight into the SOA formation rate.

The BC mixing state after this initial coating growth phase is characterized by very little change in $m_{R,100}$, which remains near 20 for 1−2 days. The reported coating thicknesses from Forrister et al.[15] and Perring et al.[17] suggest that the timing of the transition from growth to loss may vary on the order of a day. As available gas-phase SOA precursors are used up, either as coating on BC particles or growth of BC-free particles, or are diluted to the point that little material is available for coating, the rate of coating growth will slow and essentially stop. However, this *absence of change in the BC particle mixing state does not rule out continued chemical processing.*

Following this microphysically idle phase, a slow but steady loss of coating material occurs and $m_{R,100}$ decreases. For the free tropospheric plumes examined here, for which cloud processing is likely to be minimal, nearly two-thirds of the accumulated coating mass is lost within a week. A simple exponential fit for the decrease in $m_{R,100}$ from the maximum value to the observed baseline is given by

$$m_{R,100}(t) = m_{R,100_\infty} + (m_{R,100_{max}} - m_{R,100_\infty})e^{-k_{loss}t} \quad (2)$$

with $m_{R,100max}$ = 20, $m_{R,100\infty}$ = 5, and loss rate constant $k_{loss} \approx$ 0.011 h^{-1} (Figure 1, where the gray-shaded region represents values of $m_{R,100}$ corresponding to values of k_{loss} that are within 50% of 0.011 h^{-1}). This expression corresponds to an initial loss rate of coating mass for $D_{BC,med}$ = 100 nm particles of 0.16 fg h^{-1} (~0.23 nm h^{-1})—a full 2 orders of magnitude less than the initial growth rate. As above, this loss rate constant will be the same for the total coating mass of the ensemble of BC-containing particles.

In contrast to fresh emissions, the variability in $m_{R,100}$ appears to be less in aged plumes, likely because atmospheric processing results in coatings that converge toward similar compositions (i.e., oxidation state rather than explicit molecular composition); that is, atmospheric (oxidative and photolytic) processing of the coating results in the loss of memory of its initial composition (or source fuel). However, as these results are based on measurements from one particular region, possibly with similar fuel sources, confirmation from other BB events would be required to draw definitive conclusions.

2.2. Framework of the Lifecycle of Tropospheric BB−BC Particles. The evolution of the mixing state of tropospheric BB−BC particles: an initial rapid growth of coating, followed by a period during which the coating mass exhibits little change, and then a slow loss of coating (Figure 1), falls naturally into a framework consisting of three regimes: (i) "local", (ii) "regional", and (iii) "global" (Figure S2). Each regime covers different spatial and temporal extents, and the dominant physical and chemical processes that affect the evolution of the BB−BC aerosol particles and their microphysical, chemical, and thus optical and hygroscopic properties differ in each of them. The local regime, when the plume is near the source, extends to ~100 km and to ages of a few hours. The regional regime extends from ~100 km to a thousand kilometers or so (continental scales) and from a few hours to a few days. The global regime extends from a thousand kilometers or so and from a few days onward. These regimes also naturally scale with various modeling efforts. In the local regime, whose spatial and temporal extents correspond to a grid cell in a GCM, LES can be used to examine the evolution of BB−BC particles. The regional regime has spatial and temporal scales that are typical of regional climate models. In the global regime, GCMs, such as E3SM (www.e3sm.org), are the natural choice.

Although these regimes, and the processes that are dominant in each, might not be representative of every BB plume, they nonetheless appear to generally capture the lifecycle of BB−BC particles in the free troposphere. The evolution of properties of BB−BC particles, specifically the mixing state, and processes that affect these properties are now discussed in terms of these regimes.

2.3. Mixing State Evolution in the Local Regime. Black carbon particles in BB plumes are mainly generated under flaming conditions and thus tend to be emitted with little associated (primary) coating material,[22] but they rapidly become thickly coated (Figure 1) by the condensation of (mainly organic) material. Oxidation of gas-phase precursors will bring about functionalization that produces lower volatility compounds that can condense on the BC particles.[23−25] Since BC aggregate rearrangement has been shown to occur during the initial coating process,[26] collapse of the fractal-like aggregates has likely occurred by the time BB aerosols are sampled by aircraft close to emissions. Scatter in $m_{R,100}$ values and in growth rates derived for individual BBOP flights shown in Figure 1 are likely due to differences in prevailing combustion conditions[27] (e.g., active flaming, smoldering, pyrolysis), source fuel,[28] and plume dilution and cooling.[29] Condensation and coagulation of BC particles with oxidized hydrophilic vapors and particles, and direct heterogeneous oxidation of the BC particles, will rapidly convert the fresh, hydrophobic BC particles to hydrophilic ones.[30,31] This conversion represents a critical step in a BC particle lifecycle, given the importance of wet removal processes to their atmospheric lifetimes.

BBOP measurements show that the processes involved in coating BB−BC particles also drive increases in the sizes of non-BC-containing BBA particles. The diameter of the size mode of BBA particles observed by Kleinman et al.[32] (Figure 19) during flight 0821b, predominately POA, increased from near 100 nm at 15 min to near 200 nm at 90 min, corresponding to an increase in the mass of nominally a factor of 8, in fair agreement with the factor of 4 for the increase in the coating mass for the ensemble of coated BC particles. As discussed by Kleinman et al.,[32] the overall particulate organic loadings normalized by CO remained relatively constant during the rapid condensational growth, suggesting concurrent processes.

2.4. Mixing State Evolution in the Regional Regime. Within hours after emission, the rapid tropospheric BB−BC particle coating growth rates shown in Figure 1 decrease as the condensable gases are exhausted or diluted to the extent that further condensation becomes negligible. Although the mixing state remains essentially constant, chemical processing of the coating can still occur, as noted above. In particular, chromophores (i.e., light-absorbing organics, also known as brown carbon, BrC) can be generated by functionalization reactions that involve nitrate addition or destroyed by reactions involving O_3 addition across double bonds (known

https://doi.org/10.1021/acs.est.2c03851
Environ. Sci. Technol. 2022, 56, 14315−14325

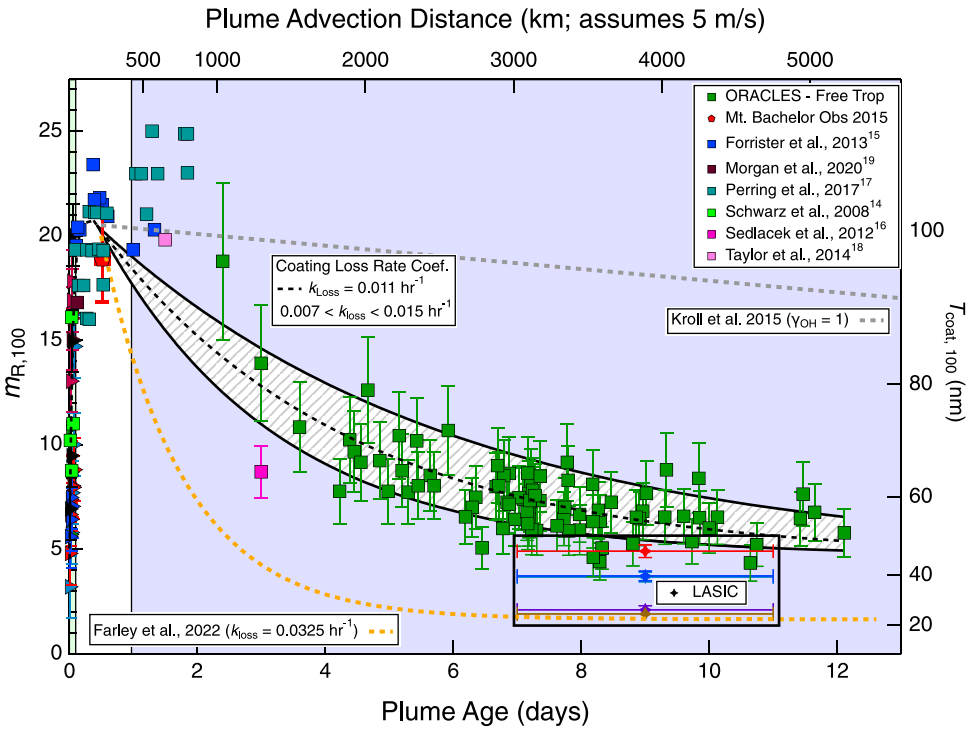

Figure 2. Same data as shown in Figure 1—mass ratio of nonrefractory coating-to-BC particles with a diameter of 100 nm, $m_{R,100}$, as a function of plume age—on a linear time scale. Linear time scale suggests that the dominant process in the BB−BC mixing state lifecycle is the loss of coating. For comparison, the gray dotted line is the squalene mass loss for a γ_{OH} of 1 from Kroll et al.[23] and the orange dotted line is the mass loss of OA measured at MBO during the 2019 wildfire season and BBOP (Farley et al.[52]). The upper axis shows plume advection distance for an assumed 5 m s^{-1} wind speed. The hashed-region captures loss rate constants that are within 50% of k_{loss}.

as bleaching), thus impacting the chemical and optical properties of these particles.[33]

2.5. Mixing State Evolution in the Global Regime. From a day or two after emission onward, the coatings on the BB−BC particles start to decrease, implying the generation of volatile products from the coating material. Four direct pathways that can bring about material loss are: (1) evaporation, (2) heterogeneous oxidation, (3) direct photolysis, and (4) aqueous-phase oxidation. Indirect pathways resulting in the apparent loss of coating material include the loss of larger, thickly coated BB−BC particles due to dry deposition or cloud processing. Recent observations strongly suggest rapid vaporization of primary BBA material in the local regime simultaneous with rapid oxidation and condensation.[32] Subsequent vaporization of secondary oxidized material in the regional to global regimes may be important, although at significantly reduced rates due to lower vapor pressures of these oxidized materials. Heterogeneous oxidation in the free troposphere occurs via OH, whereas O_3 and NO_3 are more important in the boundary layer.[34] Daytime OH and/or O_3 oxidation[35] of the coating continues after emission; nighttime oxidation by NO_3 also occurs, though it may be limited by low NO_x concentrations.[36] Direct photolysis[37] could result in fragmentation and consequent loss of coating mass but requires light-absorbing chromophores (i.e., BrC[38]). O'Brien and Kroll[39] predict photolytic aging of secondary organic aerosol to be limited to the first day or so of aging. Recent work conducted on African BB plumes[40] also suggests that extensive bleaching occurs within a few days, thus relegating the loss of coating by the direct photolysis mechanism to a secondary role. For plumes that have been entrained into the boundary layer, aqueous-phase oxidant chemistry[41] and photolytic reactions[42,43] can occur in cloud droplets or deliquesced particles, resulting in decreased particulate mass and thus a change in the BC particle mixing state. However, this reaction will be of minor importance in the current discussion, which pertains to BB plumes in the free troposphere.

Another loss mechanism suggested by Taylor et al.[20] (2020) to explain their observation that derived $m_{R,100}$ values during the CLARIFY campaign were ∼38% lower at the surface than at altitude near 5 km is the decrease in ammonium nitrate volatility with decreasing temperature (and thus increasing elevation). However, as most of the BB−BC coating is SOA, and nitrate mass concentrations were similar to BC mass concentrations,[44] there would have been insufficient nitrate to explain the observed mass loss. Additionally, while this mechanism may occur to some extent, both HYSPLIT back trajectory calculations and WRF-Chem model results indicate that the plumes at higher elevations sampled near Ascension Island were younger than those at lower altitudes, suggesting that the differences in $m_{R,100}$ may have been due to plume age, as argued here, rather than solely thermodynamic properties and processing of the aerosol.

Therefore, for free tropospheric plumes, the main process driving coating loss in the global regime is heterogeneous oxidation by OH. The rate at which this occurs can be estimated by calculating the flux of OH molecules upon a particle, equal to 1/4 the product of the mean molecular speed (∼5.8 × 10^2 m s^{-1}), the OH concentration[45] (∼1.5 × 10^{12} molecules m^{-3}), the surface area of the particle, and a correction factor that depends on the diffusivity of OH and the diameter of the particle. For a particle with $m_{R,100}$ near 20, for which the coating thickness is near 100 nm (Figure 1) and thus

https://doi.org/10.1021/acs.est.2c03851
Environ. Sci. Technol. 2022, 56, 14315−14325

the total diameter of the particle is near 300 nm, the surface area is ~2.8 × 10^{-13} m^2, and the correction factor is approximately 0.6, yielding a rate of collisions with OH molecules of ~24 s^{-1} or ~0.88 × 10^5 collisions h^{-1}. The fitted rate of decrease in $m_{R,100}$ from its maximum value is ~0.16 h^{-1} (from eq 2), and as the mass of the BC core for $D_{BC,med}$ = 100 nm is approximately 1 fg, the rate of decrease of the coating mass is ~0.16 fg h^{-1}. Under the assumption that the coating consists of organic molecules with an average molecular weight of 400 g mol^{-1}, the initial loss rate is ~2.4 × 10^5 molecules h^{-1}, which would imply a reaction efficiency γ_{OH} of ~1.8. Laboratory experiments have found the reactive uptake coefficient of OH (i.e., ratio of reactions to OH strikes on the surface of a particle) of OH to typically fall between 0.1 and 1.0, with some observations of values greater than unity, possibly due to secondary chemistry.[23,25,46,47]

The observed loss rate of more than 50% over a week is significantly faster than that observed by Kroll et al.[23] for laboratory experiments and more in agreement with the single measurement available at that time for loss rates from BB plumes from West Africa (Figure 9 of Kroll et al.[23]). A normalized mass fraction loss rate from Kroll et al.[23] for γ_{OH} of 1 is included in Figure 2 for comparison purposes, where plume age is plotted on a linear scale. Their loss fraction is based on carbon only, whereas the measured mass loss fractions presented here are not limited to carbon. This difference likely does not account for the observed mass loss rate discrepancy. Potential explanations for this large discrepancy may be related to coating thicknesses,[46] especially for larger diameter rBC particles (Figure S1) not directly included in Figure 2 (limited to diameter 100 nm). Other chemical and physical differences may be relevant. For example, the Kroll et al.[23] laboratory experiments were conducted on pure, single organic compound particles with higher than atmospheric levels of OH radicals to map out their effective "plume age", which may not fully represent atmospheric reactions.[48] In contrast, the initial heavily coated ambient BB−BC particles in Figure 2 already consist of a complex mixture of oxidized secondary organic and inorganic components, which may significantly enhance fragmentation pathways.[49] Other important aspects affecting the measured atmospheric heterogeneous oxidation of BB−BC particles that were not considered in this simple comparison include particle phase and relative humidity and the presence of other atmospheric oxidants (e.g., NO_3 and O_3) playing a role.[50,51]

Farley et al.[52] have recently reported the mass loss of BBOA in very aged Siberia smoke plumes. The observed loss was attributed to three possible processes: (i) continuing evaporation of volatile BB−POA, (ii) OA loss via deposition, and (iii) heterogeneous oxidation or loss of BB−SOA via evaporation or fragmentation reactions. Their reported mass loss rate constant for all BBOA is about 3× faster than that derived in the present study for BBA on BC particles. Comparison of the rates of mass loss from the present study and from MBO with OA mass loss reported by Kroll[23] suggests that the model systems used in the laboratory are not yet capturing the complexities present in ambient OA. Nonetheless, it is clear that OA mass is lost as these particles age in the troposphere.

A relevant question is how these observed mass loss rates match with model representations of BB aging. Schill et al.[53] report measurements of widespread biomass burning particles throughout the remote troposphere from NASA's Atmospheric Tomography Missions (ATom) and compare these concentrations with global model results. They report that the global models overestimate BBA mass concentrations by >400%, which they attribute to the under-representation of wet removal processes.[52] The extent to which heterogeneous oxidation of BBA, including BB−BC, is understood and represented in global models will impact our ability to model mass loss rates, as measured here, and wet removal rates, as well as BB−BC radiative impacts.[12]

That BC particles retain an appreciable portion of their coating even at ages greater than a week (Figures 1 and 2) suggests that this remaining material is of very low volatility and resistant to further oxidation by OH.[54] While change in SOA volatility with atmospheric processing (aging) continues to be an active area of research,[24,38,55] it has been established that oligomerization can occur, resulting in compounds that are essentially nonvolatile. Additionally, at lower temperatures, SOA can become glassy and viscous, which will also bring about a reduction in material volatility.[51,54] It is likely that one (or more) of these processes occurred for the residual coating material on the BC particles.

Eventual removal of BC from the troposphere (not shown in Figures 1 or 2) occurs through wet deposition, which depends on particle hygroscopicity, cloud amount, and precipitation rates or dry deposition, which will depend primarily on particle size. For precipitation that evaporates below clouds, BC particles are resuspended back to the aerosol phase, although generally with larger $D_{BC,med}$ due to scavenging of more than one BC-containing particle per drop.

2.6. Dominant Process of the BB−BC Particle Mixing State Lifecycle. When the evolution of the BB−BC mixing state is presented on a linear time scale (Figure 2), in contrast to the logarithmic scale (Figure 1), the relative importance of the evolution processes—coating growth to material loss—comes into clearer focus. Indeed, displaying the evolution of $m_{R,100}$ on the linear scale clearly establishes that *the process that dominates the BB−BC mixing state over the vast majority of its lifecycle is coating loss* (purple-shaded rectangle). The local regime (green-shaded rectangle) comprises only a minuscule fraction of the lifecycle of these particles: ~2 h out of 2 weeks, or less than 1%, and even the regional regime (white-shaded rectangle) is short-lived (~10%). Therefore, parameterizations that characterize BB−BC particles in regional and global models based on observations or measurements in the local regime fail to accurately capture the majority of the lifecycle of these particles.

2.7. Implications for Aerosol Optical Properties. Changes in the mixing state of BB−BC particles will drive concomitant changes in the optical properties of these particles and thus in the radiative forcing by BBA. These changes are quantified in terms of the absorption enhancement, MAC, and SSA_{BC}, calculated at a wavelength of 500 nm for the size distribution given above. The absorption enhancement starts at ~1.4 near the fire ($m_{R,100}$ near 5) and increases to near 1.7 at $m_{R,100}$ = 20 before decreasing back to near 1.4 for $m_{R,100}$ = 5 at long times. For a MAC of uncoated BC particles[1] of 7.5 m^2 g^{-1}, these absorption enhancements correspond to an increase in the MAC from ~10.3 m^2 g^{-1} near the fire to slightly greater than 12.8 m^2 g^{-1} for $m_{R,100}$ = 20, followed by a decrease back to ~10.3 m^2 g^{-1} at long times. Similarly, because an increase in coating thickness will cause a larger increase in scattering than in absorption, the initial rapid growth of coating during the first hour will result in a parallel increase in SSA_{BC}, from ~0.45

https://doi.org/10.1021/acs.est.2c03851
Environ. Sci. Technol. 2022, 56, 14315−14325

near the plume to ∼0.75 for $m_{R,100}$ near its maximum value, before dropping to ∼0.45 at long times.

As BC particles likely provide the dominant contribution to absorption for BB plumes (which include both particles that contain BC and those that do not), changes in SSA_{BC} will drive changes in the overall plume SSA, as observed in recent airborne and ground-based field campaigns. For example, during the BBOP campaign, the SSA initially increased from ∼0.8 to ∼0.9 as the plume evolved over the first few hours.[52,56] In ORACLES, a maximum value of SSA near 0.9 was derived for a less aged BB plume (∼4 days old) sampled just off the African coast, while SSA values were near ∼0.83 for African BB plumes[44,57] after ∼10 days. A similar SSA of 0.85 was reported by Wu et al. (2020),[58] who sampled BB plumes arriving at Ascension Island that were approximately a week old during the CLARIFY campaign. A minimum value of SSA of ∼0.80 was reported by Zuidema and co-workers[59] during the Ascension Island ground-based LASIC campaign, although this value was derived for boundary layer air, potentially suggesting that some additional processing had occurred that was not present in the free tropospheric plumes. An SSA of 0.85 was reported by Holanda et al. (2020)[60] for an estimated 10 day old African BB plume that had transported across the Atlantic to Brazil, which contrasted with local Brazilian fires, which had an SSA near 0.9. It is interesting to note that the agreement of the overall SSA reported by Holanda et al. (2020)[60] with those of Wu et al. (2020),[58] Dobracki et al. (2022),[44] and Pistone et al. (2019)[57] suggests that the processing responsible for the decrease in SSA_{BC} with age does not continue indefinitely, consistent with our observation of extremely low volatility coatings on very aged BC particles following a more pronounced period of coating loss.

Use of the BB−BC mixing state as a proxy for non-BC-containing BBA can be used to investigate the amount of absorption from BrC. As the same processes that determine the loss of mass from BC-containing particles would operate on particles not containing BC, these latter particles would be expected to exhibit a similar loss of mass. This inference is consistent with 2016−2017 ORACLES observations reported by Dobracki et al. (2022)[44] on the loss of BBA mass (via OA/BC ratio) as a function of plume age. Their parameterization (SSA = 0.801 + 0.0055 × OA/BC at 530 nm wavelength), with an estimated OA/BC ratio of 8.2 for a 10 day old plume (Figure 8a of their paper), yields 0.85 for the overall SSA. Using SSA_{BC} of ∼0.45 derived from our simple condensation model for a 10 day old plume yields an estimate for the SSA for OA, SSA_{OA}, of ∼0.95 (Supporting Information), suggesting the possibility of some BrC absorption. Taylor et al. (2020)[20] reported a ∼10% contribution of absorption from BrC at 405 nm for flights conducted over Ascension Island. Using the PSAP (λ = 470, 530, and 660 nm), reported absorption Angstrom exponents ranged from 1.2 near the African coast to 1−1.1 further from the coast, consistent with a low contribution from BrC.

2.8. Impact of Transportation Pathway on BB−BC Mixing State. BC particles produced by biomass burns are also observed in the upper troposphere[53] and lower stratosphere,[61] where they represent an appreciable fraction of the particles there. BB−BC particles present in the lower stratosphere[61] are characterized by very thick coatings, with $m_{R,100}$ near 50 (corresponding to a coating thickness of more than 150 nm for $D_{BC,med}$ = 100 nm)—two to three times larger than the values typical of tropospheric BB−BC particles (Figure 1). Although organic material that has condensed on the particles is the principal component of the coatings near the plume, it is likely that the dominant component of these thicker coatings is sulfuric acid, a major component in the stratosphere.[62] Ditas et al.[61] speculated that weaker removal processes and longer lifetimes in the lower stratosphere are responsible for the growth of thicker coatings. In contrast to the nominal ∼1 week that characterizes lifetimes in the free troposphere,[63] lower stratospheric lifetimes are several months,[64] thereby providing the time necessary for condensation to yield the observed sizes. The differences between the mixing states and lifetimes of BB−BC particles in the free troposphere and those in the lower stratosphere, shown schematically in Figure 1, suggest that different model representations of BB−BC particle evolution should be employed for these two transportation pathways.

2.9. Inferring BBA Evolution from BB−BC Mixing State Evolution. The central tenet in the analysis presented here is that the chemically inert and nonvolatile properties of the BC core can be exploited as a tracer to study the growth or loss of the nonrefractory coating. The temporal behavior of the coated BC particles can also be used to provide information about the growth and shrinkage of coemitted non-BC-containing BB particles, as the coating of BC-containing particles and the composition of condensates on the coemitted non-BC-containing particles will almost certainly be the same and thus will have similar chemical reactivity, hygroscopicity, optical properties (i.e., refractive index), and volatility. This compositional equivalence enables top-level observations on the BBA lifecycle to be drawn. For example, the rapid coating growth phase that characterizes the local (or source) regime suggests that non-BC-containing particles would experience a similar growth in size, allowing SOA formation rates to be determined. Additionally, Lim et al.[46] have shown that loss rates of organic coatings on top of an organic core were comparable to material loss rates observed with the pure particle analog of the coating material, lending further support for the use of the BB−BC mixing state proxy to non-BC-containing BBA aging.

3. SUMMARY

The lifecycle of biomass burning BC-containing particles is examined by combining field measurements of their mixing states in BB plumes of different ages in various regions of the world with previously published data. The BB−BC particle mixing state offers the unique opportunity to understand the magnitudes and effects of atmospheric aging processes—specifically secondary aerosol formation and processing, and the effects of these aging processes on optical properties and radiative forcing. The mass ratio of coating to BC core for particles with $D_{BC,med}$ = 100 nm, which can be experimentally determined with an SP2, provides a proxy for the BC mixing state, and a simple model is used to yield results for the mass of coating to BC core and for optical properties of the ensemble of BB−BC aerosol. Together, these temporally disparate measurements provide a coherent picture of BB−BC evolution and demonstrate for the first time that the BB−BC particle mixing state remains highly dynamic throughout the lifetime of these particles. The temporal behavior observed in the microphysical properties of BB−BC particles suggests a natural partitioning of the BC mixing state lifecycle into three regimes: local, regional, and global, which correspond to temporal and spatial scales characteristic of modeling efforts.

https://doi.org/10.1021/acs.est.2c03851
Environ. Sci. Technol. 2022, 56, 14315−14325

Following the rapid initial growth from the condensation of organic vapors near the fire and passing through to a quiescent period where there is little change in the mixing state, the coated BC particles then enter a phase where ∼75% of the coating is lost through much slower processes. Coating loss dominates the evolution of the microphysical properties as the BC-containing particles continue to age. The optical properties of these particles, and thus the radiative properties of the BBA plume, undergo similar evolutions, which are not accurately captured in regional and global models that use parameterizations based on measurements of BB−BC aerosols early in their lifecycle.

As BC is chemically inert and nonvolatile, it serves as a conservative tracer, whereby changes in the BC mixing state will be due solely to changes in the amount of nonrefractory material (i.e., coating thickness). The local regime is characterized by a rapid growth in coating due primarily to SOA formation. Following this coating growth phase, with the injection of BB−BC particles into the free troposphere, the available loss mechanisms for BC—wet and dry deposition—are reduced, enabling continued exploitation of the conserved tracer properties of BC. This exploitation reveals that as the BB−BC particles continue to age beyond ∼2−3 days, much of the coating material is lost, likely due to heterogeneous oxidation and other secondary reactions.[16,36] Such changes in coating thickness will directly impact not only the optical properties of the BB-containing particles but also the overall BBA plume, as BC remains the primary absorbing species whose absorption efficiency will drive the SSA of the BB plume.

The results presented here—that the amounts of coating material on BB−BC particles change throughout their lifetimes, as do the hygroscopic and optical properties, and thus the contribution of these particles to radiative forcing—provide a compelling argument that the current treatment of BC in GCMs does not accurately capture the processes driving BB−BC evolution and the radiative impacts of BBA plumes, and underscore the need for a re-evaluation of the use of near-field observations and experiments as the sole sources for regional and global model parameterizations.

■ ASSOCIATED CONTENT

Supporting Information

The Supporting Information is available free of charge at https://pubs.acs.org/doi/10.1021/acs.est.2c03851.

Additional information on the experimental methods, the condensation model, and on the calculation of the single scattering albedo of organic aerosol (SSAOA) (PDF)

■ AUTHOR INFORMATION

Corresponding Author

Arthur J. Sedlacek, III − *Brookhaven National Laboratory, Upton, New York 11973, United States;* orcid.org/0000-0001-9595-3653; Email: sedlacek@bnl.gov

Authors

Ernie R. Lewis − *Brookhaven National Laboratory, Upton, New York 11973, United States*

Timothy B. Onasch − *Aerodyne Research, Inc., Billerica, Massachusetts 01821, United States;* orcid.org/0000-0001-7796-7840

Paquita Zuidema − *University of Miami, Miami, Florida 33149, United States*

Jens Redemann − *University of Oklahoma, Norman, Oklahoma 73072, United States*

Daniel Jaffe − *University of Washington/Bothell, Bothell, Washington 98011, United States;* orcid.org/0000-0003-1965-9051

Lawrence I. Kleinman − *Brookhaven National Laboratory, Upton, New York 11973, United States*

Complete contact information is available at: https://pubs.acs.org/10.1021/acs.est.2c03851

Author Contributions

A.J.S., E.R.L., and T.B.O. interpreted the data and wrote the manuscript. A.J.S. was responsible for SP2 analysis. J.R. and P.Z. were PIs for ORACLES, P.Z. was PI for LASIC, and D.J. is the lead scientist for the Mount Bachelor Observatory.

Funding

This research was performed under the sponsorship of the U.S. DOE Office of Biological & Environmental Sciences (OBER) Atmospheric Research Program (ASR) under contract DE-SC0012704 (BNL) and National Aeronautics and Space Administration (NASA) under contracts NNA16BDD59I (BNL) and NNA168BD591 (BNL). A.J.S., J.R., and P.Z. gratefully acknowledge the support for the ORACLES under NASA's Earth Science Division and managed through the Earth System Science Pathfinder Program Office (grant no. NNH13ZDA001N-EVS2). P.Z. acknowledges support from grants DE-SC0021250, DOE ASR DE-SC0018272, and NASA NNX15AF98G. T.B.O. acknowledges support from the DOE ARM program during BBOP and the DOE ASR program for BOP analysis (DE-SC0014287). D.J. acknowledges the DOE ARM Climate Research program (contract number: 2016-6828) for use of their Single-Particle Soot Photometer (SP2) for the Mount Bachelor Observatory (MBO) measurement campaign.

Notes

The authors declare no competing financial interest.

All data used in the present analysis are publicly available on the Department of Energy ARM data archive (http://www.archive.arm.gov/armlogin/login.jsp). DOE ARM verifies data quality through quality assurance and data quality quality checks. Archived NASA data are available at (doi=10.5067/Suborbital/ORACLES/P3/2017_V2 and doi=10.5067/Suborbital/ORACLES/P3/2018_V2).

■ ACKNOWLEDGMENTS

The researchers recognize the DOE Atmospheric Radiation Measurement (ARM) Climate Research program and facility for the support to carry out the BBOP and LASIC campaigns. The Mt. Bachelor Observatory was supported by the National Science Foundation (award #1829893). The authors gratefully acknowledge the skill and safety exemplified by the DOE ARM G1 and NASA ORION P3 pilots and flight staff and Elizabeth Karapetyan for her work in performing the HYSPLIT calculations for the LASIC field campaign. The authors thank Tiffany Bowman for assistance with graphics.

■ ABBREVIATIONS

ASI	Ascension Island
BB	biomass burning
BBA	biomass burning aerosol

BC	black carbon
BB-BCs	biomass burning black carbon
BBOP	Biomass Burning Observation Project
HYSPLIT	HYbrid Single-Particle Lagrangian Integrated Trajectory
med	mass-equivalent diameter
LASIC	Layered Atlantic Smoke Interactions with Clouds
SOA	secondary organic aerosol
MAC	mass absorption cross section
MBO	Mount Bachelor Observatory
ORACLES	ObseRvations of Aerosols above Clouds and their intEractionS
SSA	single scattering albedo
SSA_{BC}	single scattering albedo for BC particles
POA	primary organic aerosol
rBC	refractory black carbon
SP2	Single Particle Soot Photometer
WRF-AAM	Weather Research and Forecasting with Aerosol Aware Microphysics
WRF-Chem	Weather Research and Forecasting with Chemistry

REFERENCES

(1) Bond, T. C.; Doherty, S. J.; Fahey, D. W.; Forster, P. M.; Berntsen, T.; DeAngelo, B. J.; Flanner, M. G.; Ghan, S.; Kärcher, B.; Koch, D.; Kinne, S.; Kondo, Y.; Quinn, P. K.; Sarofim, M. C.; Schultz, M. G.; Schulz, M.; Venkataraman, C.; Zhang, H.; Zhang, S.; Bellouin, N.; Guttikunda, S. K.; Hopke, P. K.; Jacobson, M. Z.; Kaiser, J. W.; Klimont, Z.; Lohmann, U.; Schwarz, J. P.; Shindell, D.; Storelvmo, T.; Warren, S. G.; Zender, C. S. Bounding the role of black carbon in the climate system: A scientific assessment. *J. Geophys. Res.: Atmos.* **2013**, *118*, 5380−5552.

(2) Jaffe, D. A.; O'Neill, S. M.; Larkin, N. K.; Holder, A. L.; Peterson, D. L.; Halofsky, J. E.; Rappold, A. G. Wildfire and prescribed burning impacts on air quality in the United States. *J. Air Waste Manage. Assoc.* **2020**, *70*, 583−615.

(3) Pardo, M.; Li, C.; He, Q.; Levin-Zaidman, S.; Tsoory, M.; Yu, Q.; Wang, X.; Rudich, Y. Mechanisms of lung toxicity induced by biomass burning aerosols. *Part. Fibre Toxicol.* **2020**, *17*, 1−5.

(4) Reid, C. E.; Brauer, M.; Johnston, F. H.; Jerrett, M.; Balmes, J. R.; Elliott, C. T. Critical Review of Health Impacts of Wildfire Smoke Exposure. *Environ. Health Perspect.* **2016**, *124*, 1334−1343.

(5) Hanes, C. C.; Wang, X.; Jain, P.; Parisien, M. A.; Little, J. M.; Flannigan, M. D. Fire-regime changes in Canada over the last half century. *Can. J. For. Res.* **2019**, *49*, 256−269.

(6) Jain, P.; Castellanos-Acuna, D.; Coogan, S. C. P.; Abatzoglou, J. T.; Flannigan, M. D. Observed increases in extreme fire weather driven by atmospheric humidity and temperature. *Nat. Clim. Change* **2022**, *12*, 63−70.

(7) Jones, M. W.; Smith, A.; Betts, R.; Canadell, J. G.; Prentice, I. C.; Le Quéré, C. *Climate Change Increases the Risk of Wildfires*; University of East Anglia https://sciencebrief.org/briefs/wildfires, 2020 (last accessed September 2022).

(8) Abatzoglou, J. T.; Williams, A. P. Impact of anthropogenic climate change on wildfire across western US forests. *Proc. Natl. Acad. Sci. U.S.A.* **2016**, *113*, 11770−11775.

(9) van der Werf, G. R.; Randerson, J. T.; Giglio, L.; Collatz, G. J.; Mu, M.; Kasibhatla, P. S.; Morton, D. C.; DeFries, R. S.; Jin, Y.; van Leeuwen, T. T. Global fire emissions and the contribution of deforestation, savanna, forest, agricultural, and peat fires (1997−2009). *Atmos. Chem. Phys.* **2010**, *10*, 11707−11735.

(10) Diamond, M. S.; Gettelman, A.; Lebosock, M. D.; McComiskey, A.; Russell, L. M.; Wood, R.; Feingold, G. To Assess marine cloud brightening's technical feasibililty, we need to know what to study – and when to stop. *Proc. Natl. Acad. Sci. U.S.A.* **2022**, *119*, No. e2118379119.

(11) Pörtner, H.-O.; Roberts, D. C.; Tignor, M. M. B.; Poloczanska, E.; Mintenbeck, K.; Alegría, A.IPCC, 2022; et al.. *Climate Change 2022: Impacts, Adaptation, and Vulnerability Contribution of Working Group II to the Sixth Assessment Report of the Intergovernmental Panel on Climate Change*, Cambridge University Press.

(12) Liu, D.; He, C.; Schwarz, J. P.; Wang, X. Lifecycle of light-absorbing carbonaceous aerosols in the atmosphere. *NPJ Clim. Atmos. Sci.* **2020**, *3*, 40.

(13) Redemann, J.; Russell, P. B.; Hamill, P. Dependence of aerosol light absorption and single scattering albedo on ambient relative humidity for sulfate aerosols with black carbon cores. *J. Geophys. Res.* **2001**, *106*, 27485−27495.

(14) Schwarz, J. P.; Gao, R. S.; Spackman, J. R.; Watts, L. A.; Thomson, D. S.; Fahey, D. W.; Ryerson, T. B.; Peischl, J.; Holloway, J. S.; Trainer, M.; Frost, G. J.; Baynard, T.; Lack, D. A.; de Gouw, J. A.; Warneke, C.; Del Negro, L. A. Measurement of the mixing state, mass, and optical size of individual black carbon particles in urban and biomass burning emissions. *Geophys. Res. Lett.* **2008**, *35*, 1−5.

(15) Forrister, H.; Liu, J.; Scheuer, E.; Dibb, J.; Ziemba, L.; Thornhill, K. L.; Anderson, B.; Diskin, G.; Perring, A. E.; Schwarz, J. P.; Campuzano-Jost, P.; Day, D. A.; Palm, B. B.; Jimenez, J. L.; Nenes, A.; Weber, R. J. Evolution of brown carbon in wildfire plumes. *Geophys. Res. Lett.* **2015**, *42*, 4623−4630.

(16) Sedlacek, A. J.; Lewis, E. R.; Kleinman, L. I.; Xu, J.; Zhang, Q. Determination of and Evidence for Non-core-shell structure of particles containing black carbon using the Single-Particle Soot Photometer (SP2). *Geophys. Res. Lett.* **2012**, *39*, 1−6.

(17) Perring, A. E.; Schwarz, J. P.; Markovic, M. Z.; Fahey, D. W.; Jimenez, J. L.; Campuzano-Jost, P.; Palm, B. D.; Wisthaler, A.; Mikoviny, T.; Diskin, G.; Sachse, G.; Ziemba, L.; Anderson, B.; Shingler, T.; Crosbie, E.; Sorooshian, A.; Yokelson, R.; Gao, R.-S. In situ measurements of water uptake by black carbon-containing aerosol in wildfire plumes. *J. Geophys. Res.: Atmos.* **2017**, *122*, 1086−1097.

(18) Taylor, J. W.; Allan, J. D.; Allen, G.; Coe, H.; Williams, P. I.; Flynn, M. J.; Le Breton, M.; Muller, J. B. A.; Percival, C. J.; Oram, D.; Forster, G.; Lee, J. D.; Rickard, A. R.; Parrington, M.; Palmer, P. I. Size-dependent wet removal of black carbon in Canadian biomass burning plumes. *Atmos. Chem. Phys.* **2014**, *14*, 13755−13771.

(19) Morgan, W. T.; Allan, J. D.; Bauguitte, S.; Darbyshire, E.; Flynn, M. J.; Lee, J.; Liu, D.; Johnson, B.; Haywood, J.; Longo, K. M.; Artaxo, P. E.; Coe, H. Transformation and ageing of biomass burning carbonaceous aerosol over tropical South America from aircraft in situ measurements during SAMBBA. *Atmos. Chem. Phys.* **2020**, *20*, 5309−5326.

(20) Taylor, J. W.; Wu, H.; Szpek, K.; Bower, K.; Crawford, I.; Flynn, M. J.; Williams, P. I.; Dorsey, J.; Langridge, J. M.; Cotterell, M. I.; Fox, C.; Davies, N. W.; Haywood, J. M.; Coe, H. Absorption closure in highly aged biomass burning smoke. *Atmos. Chem. Phys.* **2020**, *20*, 11201−11221.

(21) Bowman, K. P.; Lin, J. C.; Stohl, A.; Draxler, R.; Konopka, P.; Andrews, A.; Brunner, D. Input Data Requirements for Lagrangian Trajectory Models. *Bull. Am. Meteorol. Soc.* **2013**, *94*, 1051−1058.

(22) Li, J.; Pósfai, M.; Hobbs, P. V.; Buseck, P. R. Individual aerosol particles from biomass burning in southern Africa: 2. Compositions and aging of inorganic particles. *J. Geophys. Res.: Atmos.* **2003**, *108* (D13), 8484.

(23) Kroll, J. H.; Lim, C. Y.; Kessler, S. H.; Wilson, K. R. Heterogeneous Oxidation of Atmospheric Organic Aerosol: Kinetics of Changes to the Amount and Oxidation State of Particle-Phase Organic Carbon. *J. Phys. Chem. A* **2015**, *119*, 10767−10783.

(24) Lambe, A. T.; Onasch, T. B.; Croasdale, D. R.; Wright, J. P.; Martin, A. T.; Franklin, J. P.; Massoli, P.; Kroll, J. H.; Canagaratna, M. R.; Brune, W. H.; Worsnop, D. R.; Davidovits, P. Transitions from Functionalization to Fragmentation Reactions of Laboratory Secondary Organic Aerosol (SOA) Generated from the OH Oxidation of Alkane Precursors. *Environ. Sci. Technol.* **2012**, *46*, 5430−5437.

(25) Smith, J. D.; Kroll, J. H.; Cappa, C. D.; Che, D. L.; Liu, C. L.; Ahmed, M.; Leone, S. R.; Worsnop, D. R.; Wilson, K. R. The heterogeneous reaction of hydroxyl radicals with sub-micron squalane

https://doi.org/10.1021/acs.est.2c03851
Environ. Sci. Technol. 2022, 56, 14315−14325

particles: a model system for understanding the oxidative aging of ambient aerosols. *Atmos. Chem. Phys.* **2009**, *9*, 3209−3222.
(26) Chen, C.; Enekwizu, O. Y.; Fan, X.; Dobrzanski, C. D.; Ivanova, E. V.; Ma, Y.; Gor, G. Y.; Khalizov, A. Single Parameter for Predicting the Morphology of Atmospheric Black Carbon. *Environ. Sci. Technol.* **2018**, *52*, 14169−14179.
(27) Collier, S.; Zhou, S.; Onasch, T. O.; Jaffe, D.; Kleinman, L. I.; Sedlacek, A. J., III; Briggs, N.; Hee, J.; Fortner, E.; Shilling, J. E.; Worsnop, D.; Yokelson, R. J.; Parworth, C.; Ge, X.; Xu, J.; Butterfield, Z.; Chand, D.; Dubey, M. K.; Pekour, M.; Springston, S. R.; Zhang, Q. Regional Influence of Aerosol Emissions from Wildfires Driven by Combustion Efficiency: Insights from the BBOP Campaign. *Environ. Sci. Technol.* **2016**, *50*, 8613−8622.
(28) Hosseini, S.; Urbanski, S. P.; Dixit, P.; Qi, L.; Burling, I. R.; Yokelson, R. J.; Johnson, T. J.; Shrivastava, M.; Jung, H. S.; Weise, D. R.; Miller, J. W.; Cocker, D. R., III Laboratory characterization of PM emissions from combustion of wildland biomass fuels. *J. Geophys. Res.: Atmos.* **2013**, *118*, 9914−9929.
(29) Hodshire, A. L.; Ramnarine, E.; Akherati, A.; Alvarado, M. L.; Farmer, D. K.; Jathar, S. H.; Kreidenweis, S. M.; Lonsdale, C. R.; Onasch, T. B.; Springston, S. R.; Wang, J.; Wang, Y.; Kleinman, L. I.; Sedlacek, A. J., III; Pierce, J. R. Dilution impacts on smoke aging: Evidence in BBOP data. *Atmos. Chem. Phys.* **2021**, *21*, 6839−6855.
(30) Dalirian, M.; Ylisirniö, A.; Buchholz, A.; Schlesinger, D.; Ström, J.; Virtanen, A.; Riipinen, I. Cloud droplet activation of black carbon particles coated with organic compounds of varying solubility. *Atmos. Chem. Phys.* **2018**, *18*, 12477−12489.
(31) Enekwizu, O. Y.; Hasani, A.; Khalizov, A. F. Vapor Condensation and Coating Evaporation Are Both Responsible for Soot Aggregate Restructuring. *Environ. Sci. Technol.* **2021**, *55*, 8622−8630.
(32) Kleinman, L. I.; Sedlacek, A. J., III; Adachi, K.; Buseck, P.; Collier, S.; Dubey, M. K.; Hodshire, A. L.; Lewis, E.; Onasch, T. O.; Pierce, J. R.; Shilling, J.; Springston, S.; Wang, J.; Zhang, Q.; Zhou, S.; Yokelson, R. Rapid Evolution of Aerosol Particles and their Optical Properties Downwind of Wildfires in the Western. U.S. *Atmos. Chem. Phys.* **2020**, *20*, 13319−13341.
(33) Hems, R. F.; Schnitzler, E. G.; Liu-Kang, C.; Cappa, C. D.; Abbatt, J. P. D. Aging of Atmospheric Brown Carbon Aerosol. *ACS Earth Space Chem.* **2021**, *5*, 722−748.
(34) Mayorga, R. J.; Zhao, Z.; Shang, H. Formation of secondary organic aerosol from nitrate radical oxidation of phenolic VOCs: Implications for nitration mechanisms and brown carbon formation. *Atmos. Environ.* **2021**, *244*, No. 117910.
(35) George, I. J.; Abbatt, J. P. D. Heterogeneous oxidation of atmospheric aerosol particles by gas-phase radicals. *Nat. Chem.* **2010**, *2*, 713−722.
(36) Palm, B. B.; Peng, Q.; Fredrickson, C. D.; Lee, B. H.; Garofalo, L. A.; Pothier, M. A.; Kreidenweis, S. M.; Farmer, D. K.; Pokhrel, R. P.; Shen, Y.; Murphy, S. M.; Permar, W.; Hu, L.; Campos, T. L.; Hall, S. R.; Ullmann, K.; Zhang, X.; Flocke, F.; Fischer, E. V.; Thornton, J. A. Quantification of organic aerosol and brown carbon evolution in fresh wildfire plumes. *Proc. Natl. Acad. Sci. U.S.A.* **2020**, *117*, 29469−29477.
(37) Zawadowicz, M. A.; Lee, B. H.; Shrivastava, M.; Zelenyuk, A.; Zaveri, R. A.; Flynn, C.; Thornton, J. A.; Shilling, J. E. Photolysis Controls Atmospheric Budgets of Biogenic Secondary Organic Aerosol. *Environ. Sci. Technol.* **2020**, *54*, 3861−3870.
(38) Andreae, M. O.; Gelencsér, A. Black carbon or brown carbon? The nature of light-absorbing carbonaceous aerosols. *Atmos. Chem. Phys.* **2006**, *6*, 3131−3148.
(39) O'Brien, R. E.; Kroll, J. H. Photolytic aging of secondary organic aerosol: Evidence for a substantial photo-recalcitrant fraction. *J. Phys. Chem. Lett.* **2019**, *10*, 4003−4009.
(40) Dang, C.; Segal-Rozenhaimer, M.; Che, H.; Zhang, L.; Formenti, P.; Taylor, J.; Dobracki, A.; Purdue, S.; Wong, P.-S.; Nenes, A.; Sedlacek, A. J.; Coe, H.; Redemann, J.; Zuidema, P.; Howell, S.; Haywood, J. Biomass burning and marine aerosol processing over the southeast Atlantic Ocean: A TEM single particle analysis. *Atmos. Chem. Phys.* **2022**, *22*, 9389−9412.
(41) Daumit, K. E.; Carrasquillo, A. J.; Hunter, J. F.; Kroll, J. H. Laboratory studies of the aqueous-phase oxidation of polyols: submicron particles vs. bulk aqueous solution. *Atmos. Chem. Phys.* **2014**, *14*, 10773−10784.
(42) Daumit, K. E.; Carrasquillo, A. J.; Sugrue, R. A.; Kroll, J. H. Effects of Condensed-Phase Oxidants on Secondary Organic Aerosol Formation. *J. Phys. Chem. A* **2016**, *120*, 1386−1394.
(43) Bateman, A. P.; Nizkorodov, S. A.; Laskin, J.; Laskin, A. Photolytic processing of secondary organic aerosols dissolved in cloud droplets. *Phys. Chem. Chem. Phys.* **2011**, *13*, 12199−12212.
(44) Dobracki, A.; Zuidema, P.; Howell, S.; Saide, P.; Freitag, S.; Aiken, A. C.; Burton, S. P.; Sedlacek, A. J., III; Redemann, J.; Wood, R. An attribution of the low single-scattering albedo of biomass-burning aerosol over the southeast Atlantic. *Atmos. Chem. Phys. Discuss.* **2022**, 1−40.
(45) Travis, K. R.; Heald, C. L.; Allen, H. M.; Apel, E. C.; Arnold, S. R.; Blake, D. R.; Brune, W. H.; Chen, Z.; Commane, R.; Crounse, J. D.; Daube, B. C.; Diskin, G. S.; Elkins, J. W.; Evans, M. J.; Hall, S. R.; Hintsa, E. J.; Hornbrook, R. S.; Kasibhatla, P. S.; Kim, M. J.; Luo, G.; McKain, K.; Millet, D. B.; Moore, F. L.; Peischl, J.; Ryerson, T. B.; Sherwen, T.; Thames, A. B.; Ullmann, K.; Wang, Z.; Wennberg, P. O.; Wolfe, G. M.; Yu, F. Constraining remote oxidation capacity with ATom observations. *Atmos. Chem. Phys.* **2020**, *20*, 7753−7781.
(46) Lim, C. Y.; Browne, E. C.; Sugrue, R. A.; Kroll, J. H. Rapid heterogeneous oxidation of organic coatings on submicron aerosols. *Geophys. Res. Lett.* **2017**, *44*, 2949−2957.
(47) Slade, J. H.; Knopf, D. A. Heterogeneous OH oxidation of biomass burning organic aerosol surrogate compounds: assessment of volatilisation products and the role of OH concentration on the reactive uptake kinetics. *Phys. Chem. Chem. Phys.* **2013**, *15*, 5898.
(48) Peng, Z.; Jimenez, J. L. Radical chemistry in oxidation flow reactors for atmospheric chemistry research. *Chem. Soc. Rev.* **2020**, *49*, 2570−2616.
(49) Chapleski, R. C.; Zhang, Y.; Troya, D.; Morris, J. R. Heterogeneous chemistry and reaction dynamics of the atmospheric oxidants, O_3, NO_3, and OH, on organic surfaces. *Chem. Soc. Rev.* **2016**, *45*, 3731−3746.
(50) Li, J.; Forrester, S. M.; Knopf, D. A. Heterogeneous oxidation of amorphous organic aerosol surrogates by O_3, NO3, and OH at typical tropospheric temperatures. *Atmos. Chem. Phys.* **2020**, *20*, 6055−6080.
(51) Knopf, D. A.; Forrester, S. M.; Slade, J. H. Heterogeneous oxidation kinetics of organic biomass burning aerosol surrogates by O_3, NO_2, N_2O_5, and NO_3. *Phys. Chem. Chem. Phys.* **2011**, *13*, 21050.
(52) Farley, R.; Bernays, N.; Jaffe, D. A.; Ketcherside, D.; Hu, L.; Zhou, S.; Collier, S.; Zhang, Q. Persistent Influence of Wildfire Emissions in the Western United States and Characteristics of Aged Biomass Burning Organic Aerosols under Clean Air Conditions. *Environ. Sci. Technol.* **2022**, *56*, 3645−3657.
(53) Schill, G. P.; Froyd, K. D.; Bian, H.; Kupc, A.; Williamson, C.; Brock, C. A.; Ray, E.; Hornbrook, R. S.; Hills, A. J.; Apel, E. C.; Chin, M.; Colarco, P. R.; Murphy, D. M. Widespread biomass burning smoke throughout the remote troposphere. *Nat. Geosci.* **2020**, *13*, 422−427.
(54) Shrivastava, M.; Zelenyuk, A.; Imre, D.; Easter, R.; Beranek, J.; Zaveri, R. A.; Fast, J. Implications of low volatility SOA and gas-phase fragmentation reactions on SOA loadings and their spatial and temporal evolution in the atmosphere. *J. Geophy. Res. Atoms.* **2013**, *118*, 3328−3342.
(55) Mikhailov, E.; Vlasenko, S.; Martin, S. T.; Koop, T.; Pöschl, U. Amorphous and crystalline aerosol particles interacting with water vapor: conceptual framework and experimental evidence for restructuring, phase transitions and kinetic limitations. *Atmos. Chem. Phys.* **2009**, *9*, 9491−9522.
(56) Sedlacek, A. J., III; Buseck, P. R.; Adachi, K.; Onasch, T. B.; Springston, S. R.; Kleinman, L. I. Formation and evolution of tar balls

from northwestern US wildfires. *Atmos. Chem. Phys.* **2018**, *18*, 11289−11301.
(57) Pistone, K.; Redemann, J.; Doherty, S.; Zuidema, P.; Burton, S.; Cairns, B.; Cochrane, S.; Ferrare, R.; Flynn, C.; Freitag, S.; Howell, S. G.; Kacenelenbogen, M.; LeBlanc, S.; Liu, X.; Schmidt, K. S.; Sedlacek, A. J., III; Segal-Rozenhaimer, M.; Shinozuka, Y.; Stamnes, S.; van Diedenhoven, B.; Van Harten, G.; Xu, F. Intercomparison of biomass burning aerosol optical properties from in-situ and remote-sensing instruments in ORACLES-2016. *Atmos. Chem. Phys.* **2019**, *19*, 9181−9208.
(58) Wu, H.; Taylor, J. W.; Szpek, K.; Langridge, J.; Williams, P. I.; Flynn, M.; Allan, J. D.; Abel, S. J.; Pitt, J.; Cotterell, M. I.; Fox, C. N.; Davies, N. W.; Haywood, J.; Coe, H. Vertical variability of the properties of highly aged biomass burning aerosol transported over the southeast Atlantic during CLARIFY- 2017. *Atmos. Chem. Phys.* **2020**, *20*, 12697−12719.
(59) Zuidema, P.; Sedlacek, A. J., III; Flynn, C.; Springston, S.; Delgadilo, R.; Zhang, J.; Aiken, A. C.; Koontz, A.; Muradyan, P. The Ascension Island Boundary Layer in the Remote Southeast Atlantic is Often Smoky. *Geophys. Res. Lett.* **2018**, *45*, 4456−4465.
(60) Holanda, B. A.; Pöhlker, M. L.; Walter, D.; Saturno, J.; Sörgel, M.; Ditas, J.; Ditas, F.; Schulz, C.; Franco, M. A.; Wang, Q.; Donth, T.; Artaxo, P.; Barbosa, H. M. J.; Borrmann, S.; Braga, R.; Brito, J.; Cheng, Y.; Dollner, M.; Kaiser, J. W.; Klimach, T.; Knote, C.; Krüger, O. O.; Fütterer, D.; Lavrič, J. V.; Ma, N.; Machado, L. A. T.; Ming, J.; Morais, F. G.; Paulsen, H.; Sauer, D.; Schlager, H.; Schneider, J.; Su, H.; Weinzierl, B.; Walser, A.; Wendisch, M.; Ziereis, H.; Zöger, M.; Pöschl, U.; Andreae, M. O.; Pöhlker, C. Influx of African biomass burning aerosol during the Amazonian dry season through layered transatlantic transport of black carbon-rich smoke. *Atmos. Chem. Phys.* **2020**, *20*, 4757−4785.
(61) Ditas, J.; Ma, N.; Zhang, Y.; Assmann, D.; Neumaier, M.; Riede, H.; Karu, E.; Williams, J.; Scharffe, D.; Wang, Q.; Saturno, J.; Schwarz, J. P.; Katich, J. M.; McMeeking, G. R.; Zahn, A.; Hermann, M.; Brenninkmeiger, C. A. M.; Andreae, M. O.; Pöschl, U.; Su, H.; Cheng, Y. Strong impact of wildfires on the abundance and aging of black carbon in the lowermost stratosphere. *Proc. Natl. Acad. Sci. U.S.A.* **2018**, *115*, E11595−E11603.
(62) Deshler, T. A review of global stratospheric aerosol: Measurements, importance, life cycle, and local stratospheric aerosol. *Atmos. Res.* **2008**, *90*, 223−232.
(63) Lund, M. T.; Samset, B. H.; Skeie, R. B.; Watson-Parris, D.; Katich, J. M.; Schwarz, J. P.; Weinzierl, B. Short Black Carbon lifetime inferred from a global set of aircraft observations. *npj Clim. Atmos. Sci.* **2018**, *1*, No. 31.
(64) Chazette, P.; David, C.; Lefrere, J.; Godin, S.; Pelon, J.; Megie, G. Comparative lidar study of the optical, geometrical, and dynamical properties of stratospheric post-volcanic aerosols, following the eruptions of El Chichon and Mount Pinatubo. *J. Geo. Phys. Res.* **1995**, *100*, 23195−23207.

https://doi.org/10.1021/acs.est.2c03851
Environ. Sci. Technol. 2022, 56, 14315−14325